Research paper

Pyrazole-based potent inhibitors of GGT1: Synthesis, biological evaluation, and molecular docking studies

Muhammad Mansha [a, b], Udayappan Udhaya Kumari [c], Zoe Cournia [d], Nisar Ullah [a, *]

[a] Chemistry Department, King Fahd University of Petroleum and Minerals, Dhahran, Saudi Arabia
[b] Center of Research Excellence in Nanotechnology, King Fahd University of Petroleum and Minerals, Dhahran, Saudi Arabia
[c] Program in Cancer and Stem Cell Biology, Duke-NUS Graduate School, 8 College Road, Singapore 169857, Singapore
[d] Biomedical Research Foundation, Academy of Athens, 4 Soranou Ephessiou, 11527 Athens, Greece

ARTICLE INFO

ABSTRACT

In this study, a series of pyrazole-based structural analogues of GGTI-DU40 (**1**) have been synthesized and biologically evaluated for geranylgeranyltransferase 1 (GGT1) and farnesyltransferase (FT) inhibition. The screening results revealed that **2** (IC_{50} = 2.4 μM) and **5** (IC_{50} = 3.1 μM) are potent GGT1 inhibitors (GGTIs), possessing higher inhibitory activity compared to the control compound **1** (IC_{50} = 3.3 μM). The anti-proliferative efficacy of these compounds was further assayed against MDA-MB-231 cells which indicated a significantly higher activity of **2** (IC_{50} = 7.6 μM) compared to **1** (IC_{50} = 23.0 μM). To examine the capacity of the synthesized compounds to inhibit GGT1 in an intact cell, western blot analysis was performed on the MDA-MB-231 cell line, which revealed very high inhibitory cellular activity of **2** and **5** and demonstrated their capacity to inhibit prenylation of endogenous proteins. Molecular docking studies of **2** against the crystal structure of GGT1 complexed with a geranylgeranyl pyrophosphate (GGPP) Analog and a CaaX (C = cysteine, aa = aliphatic amino acids, and X = any amino acid) portion of the KKKSKTKCVIL peptide substrate revealed several hydrogen bonding interactions and π-π contacts between **2** and the binding pocket of GGT1. Together these data suggest that compound **2** could proceed to in vivo investigation to further assess its efficacy and cytotoxicity.

© 2016 Elsevier Masson SAS. All rights reserved.

1. Introduction

Protein prenylation is one of the most crucial post-translational modifications in biology that determines subcellular membrane localization, which in turn can influence effector binding or activation and regulatory protein interactions [1]. The Ras superfamily of small GTPases is the largest protein family that is regulated through post-translational prenylation for its spatio-temporal activation [2]. The majority of GTPase prenylated proteins contain a C-terminal CaaX sequence. The CaaX motif serves as the substrate for prenylation, which involves covalent addition of either farnesyl (15-carbon unit, added when X = Ser, Ala, or Met) or geranylgeranyl (20-carbon unit, added when X = Leu) isoprenoids to the cysteine side-chain thiol near the C-terminus of a target protein. These modifications are catalyzed by the FT and GGT1 proteins, which attach the 15- and 20-carbon isoprenoid lipids to CaaX motifs,

respectively [3]. After the covalent attachment of the isoprenoid in the cytoplasm, the majority of CaaX proteins undergo two further prenylation-dependent processing steps: proteolytic removal of the aaX tripeptide by the CaaX protease Rce1 followed by the carboxymethylation of the prenylcysteine residue by the isoprenylcysteine carboxyl methyltransferase (Icmt) [4]. The fully processed prenylated CaaX proteins such as Ras proteins, GTPases, RhoC, and Ra1, exhibit high affinity for cellular membranes and play critical roles in a wide variety of cellular processes, including transmembrane signaling, membrane trafficking and nuclear events [5].

The contribution of the Ras family members, particularly K-Ras, to human tumorigenesis [6], the widespread GTPase activation in cancer [7], the major contribution of RhoC to metastasis of some solid tumors [8,9] and Ral proteins activation in more than 90% of pancreatic duct adenocarcinoma cases, triggered interest in identifying inhibitors of prenylation enzymes as anti-cancer agents [10]. Early studies focused on the development of FT inhibitors (FTIs) due to the FT involvement in Ras maturation and oncogenic activity. While FTIs were efficacious in in vitro and in vivo preclinical studies

---

* Corresponding author.
  E-mail address: nullah@kfupm.edu.sa (N. Ullah).

of malignancies, they did not show efficacy in clinical trials [5], perhaps in part due to alternate geranylgeranylation mechanisms of N-Ras and K-Ras by GGT1 when FT is inhibited [11]. Thus, the GGT1 implication in cancer has received much attention in recent studies. The GGT1 deficiency has been implicated in proliferation inhibition and accumulation of p21CIP1/WAF1 and reduction of the oncogenic K-Ras-induced lung tumor formation in mice [12]. Moreover, geranylgeranylated proteins such as Rho, Rac and Cdc42 have been linked to tumorigenesis and metastasis [13–15]. In addition, GGT1 inhibition can cause cell cycle arrest at G0/G1 [16,17], stimulate apoptosis in multiple cell lines [18–20] and was found to regress breast tumor xenografts in vivo [21]. The implications of geranylgeranylated proteins in oncogenesis have highlighted the potential of GGTIs as promising chemotherapies [2,22]. Consequently, different strategies have been explored to develop GGTIs [23], including peptidomimetic and small-molecules inhibitors [24–26].

A recent focus of our work has been the synthesis of molecules of medicinal value [27]. Driven by the limited bioavailability of a potent and selective inhibitor of GGT1 (DU40) both *in vitro* and in living cells, associated with its hydrophobicity, we were motivated to design a series of substituted pyrazoles **2–16** (Fig. 1) [26]. Herein, we wish to disclose the synthesis and biological evaluation of compounds **2–16** and molecular docking studies of the most active compound **2** in the series.

2. Results and discussion

2.1. Chemistry

The synthesis of compounds **2–16** necessitated the preparation of suitably modified amino acid derivatives. As outlined in Scheme 1, esterification of amino acids **17–19** produced the corresponding amino esters **20–22** [28–30]. Likewise, acid-induced removal of Boc protection of ester **23** [31], produced the amino ester **24** in 98% yield [32]. Moreover, reaction of amino esters **20–22** and **24** with ammonium hydroxide in a pressure vessel heating at 100 °C overnight produced the desired α-amino amides **25–28** in good to

excellent yields (85–95%) [33] (see Scheme 2).

Similarly, amino acids **29–32** were transformed to the corresponding N-acetylated amino acids (**33**, **35**, **37** and **39**) by acetylation with acetic anhydride in MeOH under reflux. N-acylated amino acids (**34**, **36**, **38** and **40**) were produced by mesylation of **29–32** with methanesulfonyl chloride (MsCl) in a mixture of CH_2Cl_2 and 1 M NaOH [34].

L-tyrosine **41** was also converted to its corresponding N-acetylated or N-acylated derivatives **42–44** by employing previously-reported procedures [35,36]. (see Scheme 3)

With the above-mentioned modified amino acids in hand, we next moved to synthesize compounds **2–5** (Scheme 4). To this end, ethyl nicotinate **45** was treated with γ-butyrolactone in ethanol using sodium ethoxide as a base to produce α-ketobutyrolactone **46** [37]. Condensation of **46** with 3,4-dichlorophenylhydrazine hydrochloride in acetic acid produced the pyrazole **47** [38]. The O-alkylation of **47** with the ethyl 4-bromobutanoate in DMF produced the pyrazole ester **48** [38], which was hydrolyzed using LiOH in a mixture of H_2O, MeOH, and THF to remove both the acetyl and ester moieties, generating intermediate **49** [38] in 42% overall yield from **47**. Next, amidation of intermediate **49** with amino acids **25–28** in a mixture of CH_2Cl_2 and DMF, using N-(3-dimethylaminopropyl)-N′-ethylcarbodiimide hydrochloride and N-hydroxybenzotriazole as coupling agents, produced the corresponding pyrazole amides **50–53** in good yields (Scheme 4).

It is worth mentioning that we first attempted to deacetylate **48** by employing milder basic conditions (K_2CO_3, MeOH) to produce the corresponsing hydroxy ester (R_1 = Et; R_2 = H). The latter was intended to be transformed to the corresponding thiomethyl ether carboxylic acid, a thioether analog of **49** (R_1 = H; R_2 = SCH_3), by mesylation of alcohol and then condensation with sodium methanethiolate and basic hydrolysis of the ester function. However, the deacetylation of **48**, led to an undesired side product that had lost the O-acetyl and ester moieties, as evident from the ^1H NMR and IR spectra. Nevertheless, mesylation of intermediates **50–53** with MsCl in CH_2Cl_2, followed by condensation of the resultant mesylate with sodium methanethiolate in DMF, produced the desired compounds **2–5** in good to high yields (67–85%).
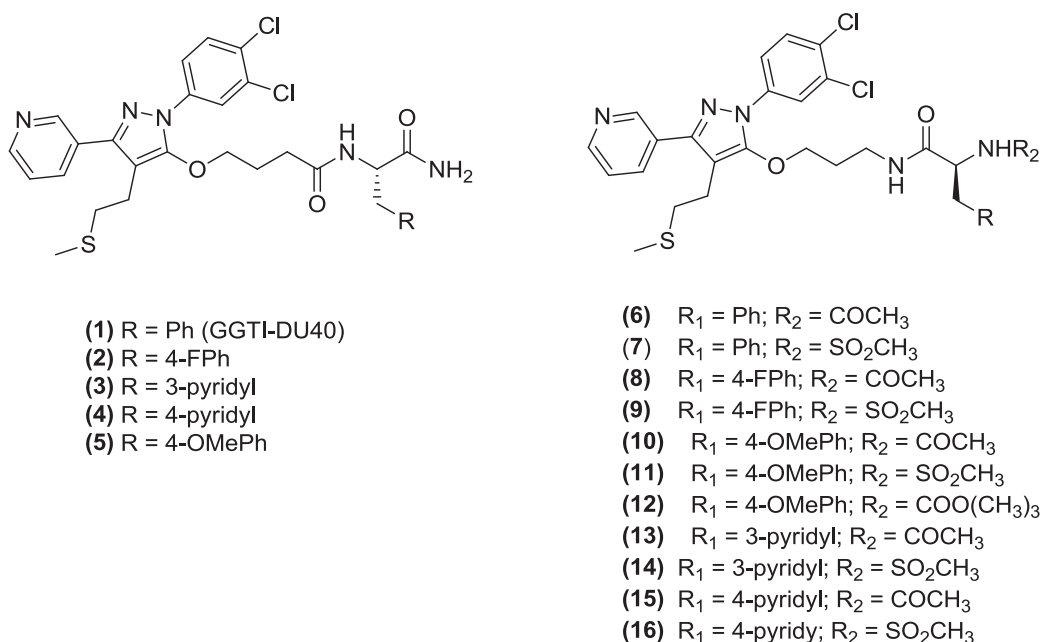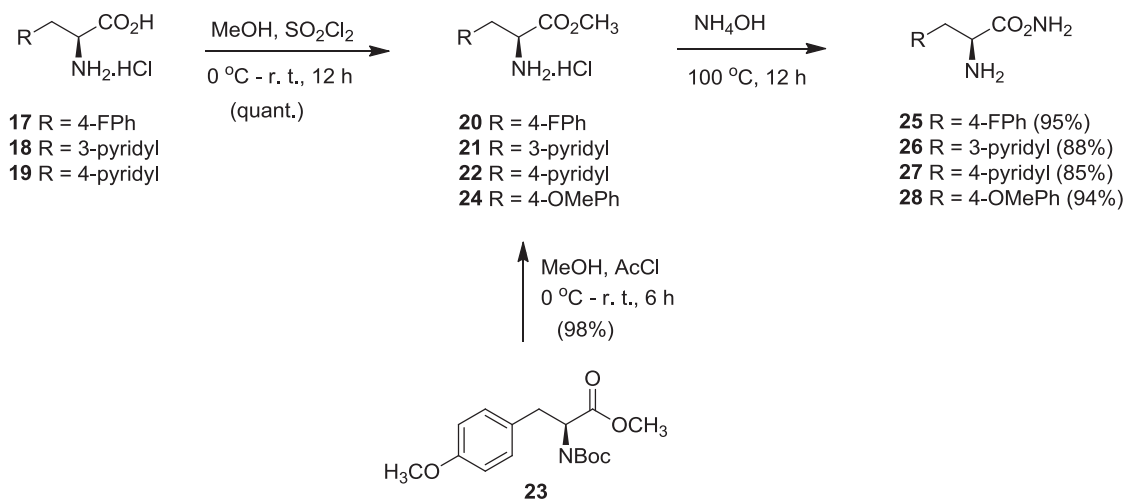

(1) R = Ph (GGTI-DU40)
(2) R = 4-FPh
(3) R = 3-pyridyl
(4) R = 4-pyridyl
(5) R = 4-OMePh

(6) R_1 = Ph; R_2 = $COCH_3$
(7) R_1 = Ph; R_2 = SO_2CH_3
(8) R_1 = 4-FPh; R_2 = $COCH_3$
(9) R_1 = 4-FPh; R_2 = SO_2CH_3
(10) R_1 = 4-OMePh; R_2 = $COCH_3$
(11) R_1 = 4-OMePh; R_2 = SO_2CH_3
(12) R_1 = 4-OMePh; R_2 = $COO(CH_3)_3$
(13) R_1 = 3-pyridyl; R_2 = $COCH_3$
(14) R_1 = 3-pyridyl; R_2 = SO_2CH_3
(15) R_1 = 4-pyridyl; R_2 = $COCH_3$
(16) R_1 = 4-pyridy; R_2 = SO_2CH_3

Fig. 1. Chemical structures of compounds **1–16**.

Scheme 1. Synthesis of amino acid derivatives **25**–**28**.
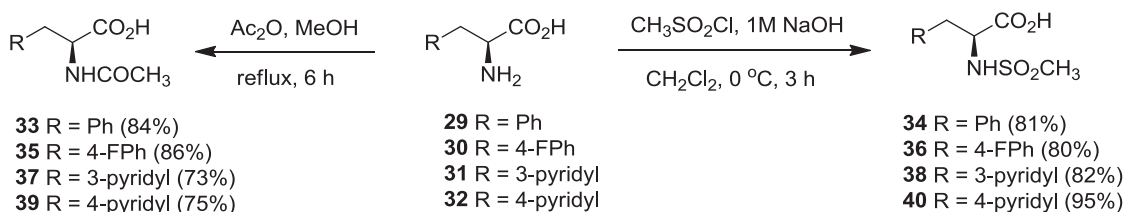
Scheme 2. Synthesis of amino acid derivatives **33**–**40**.
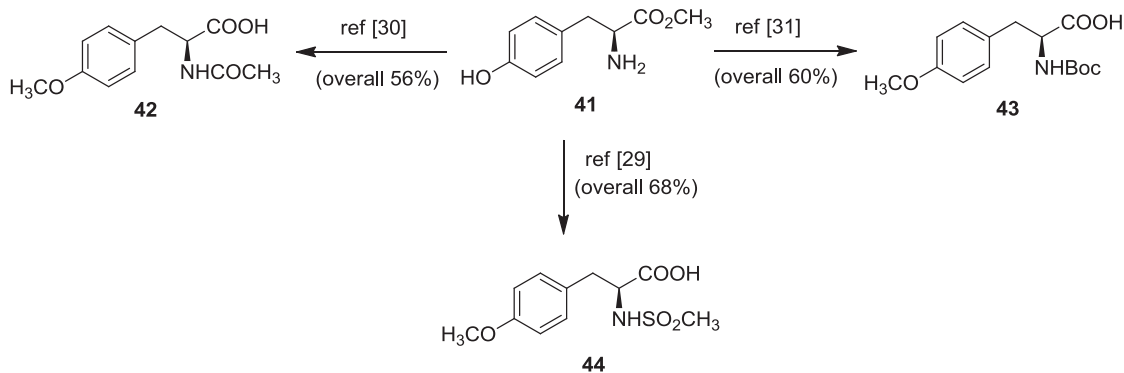
**Scheme 3.** Synthesis of amino acid derivatives **42**–**44**.

Synthesis of compounds **6**–**16** [34] was ensued as outlined in Scheme 5. In brief, the O-alkylation of pyrazole **47** with *tert*-butyl (3-bromopropyl)carbamate in DMF at room temperature produced the desired intermediate **54**, which was in turn subjected to basic hydrolysis to produce alcohol **55**. Mesylation of **55** constructed **56**, which was condensed with sodium methanethiolate in DMF to yield the thioether **57**. The acid-induced removal of Boc protection with acetyl chloride in MeOH produced the desired primary amine **58** in 64% overall yield from **54** (Scheme 5). The amidation of the primary amine **58** with **33**–**40** and **42**–**44** finally rendered access to **6**–**16** in moderate to good yields (57–69%) [34].

2.2. Biological results

2.2.1. GGT1 and FT assays

All the synthesized compounds (**2**–**16**) were screened for *in vitro*

inhibition against recombinant purified GGT1 and FT, using GGTI-DU40 (**1**) and FTI-277 as positive controls, respectively. The screening results are summarized in Table 1. For the GGT1 inhibition assay, we observed a clear trend of decreased inhibitory activity for propanamides (**6**–**16**), which were derived from the coupling of propanoxypyrazole propanamine with suitably modified amino acid derivatives, compared to butanamides (**2**–**5**), which originated from the reaction of propanoxypyrazole butanoic acid with α-amino amides. Compound **11** (IC$_{50}$ = 9.9 μM) that bears a 4-methoxyphenyl ring on the amino acid, turned out to be the most active in the propanamide series. The activity decreased more than three-fold when the N- methylsulfonamido moiety of **11** was substituted with an acetamido moiety to produce **10** (IC$_{50}$ = 34.8 μM). The influence of N-methylsulfonamido group in the enhanced activity of the propanamide series was further evident when the activity of **9** (IC$_{50}$ = 19.7 μM), bearing a 4-
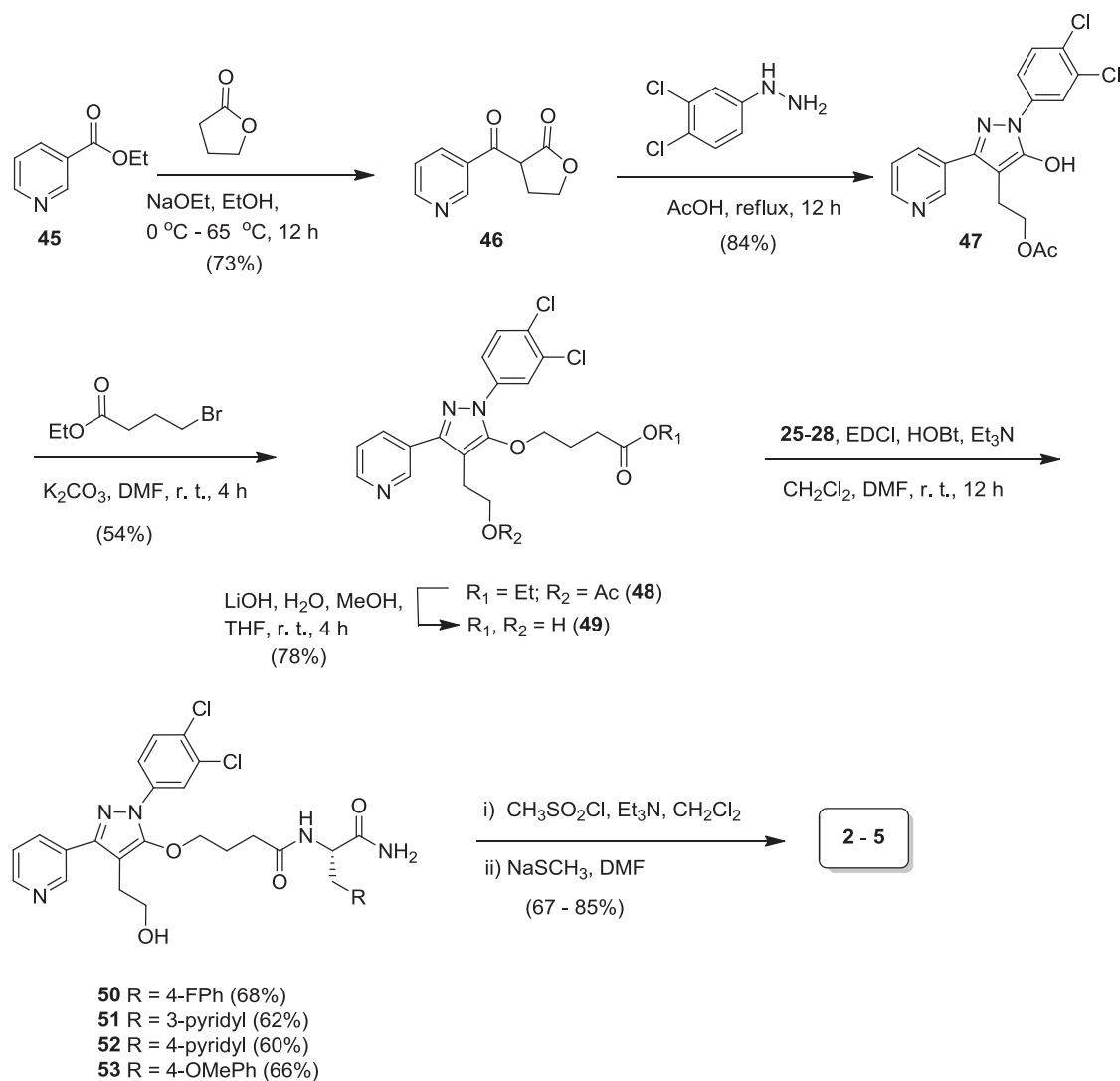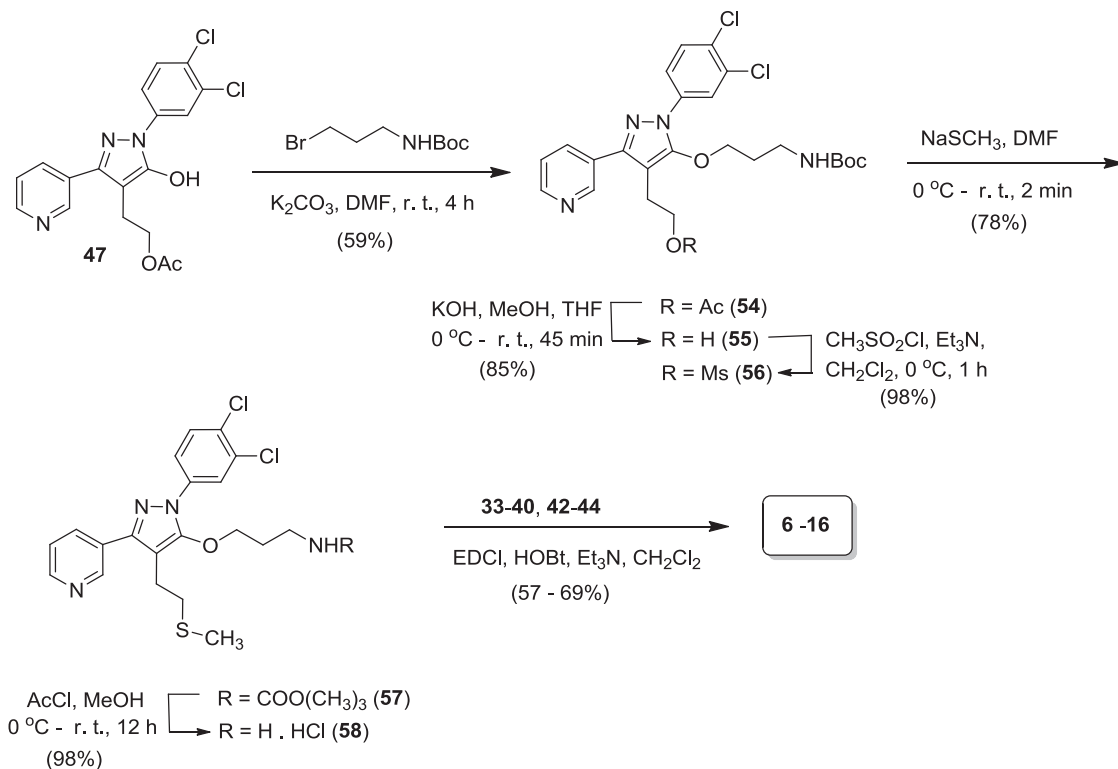
Scheme 4. Synthesis of **2**–**5**.

fluorophenyl ring on the amino acid, was slightly reduced compared to its acetamido counterpart **8** (IC$_{50}$ = 26.3 μM). Comparison of inhibitory activities of **9** and **11** revealed that the 4-methoxyphenyl on the amino acid is more crucial compared to the corresponding 4-methoxyphenyl moiety. In fact, the activities of propanamides were totally lost or diminished significantly when the combination of either 4-methoxyphenyl or 4-fluorophenyl on the amino acid and the N-methylsulfonamido group were absent. For instance, whereas compounds **6** (IC$_{50}$ = 22.9 μM), **7** (IC$_{50}$ = 31.9 μM), **15** (IC$_{50}$ = 26.9 μM) and **16** (IC$_{50}$ = 19.0 μM) had moderate activities, compounds **12**–**14** turned out to be completely inactive (Table 1).

It is apparent that the nature of the linker connecting the pyrazole moiety and the amino acid played a significant role in the activities of **2**–**5** compared to **6**–**16**. Compound **2** (IC$_{50}$ = 2.4 μM) that was produced by incorporating the fluoro group at C-4 of the amino acid phenyl ring of **1** turned out to be the most active in the series, showing higher activity than **1** (IC$_{50}$ = 3.3 μM). An earlier report has suggested that placing a fluorine at the para position of the phenyl ring (C-4) has significantly enhanced the activity of a thrombin inhibitor compared to when it was present at other positions of the phenyl ring. This high potency was attributed to the dipolar C−F···H−C$_\alpha$ and C−F···C=O interactions between the 4-fluorophenyl ring and the enzyme's active site [39]. The role of 4-fluorophenyl ring in the high potency of compound **2** was evident with the observation that when it was replaced with pyridyine-3-yl or pyridyine-4-yl group to produce **3** (IC$_{50}$ = 11.6 μM) and **4** (IC$_{50}$ = 7.8 μM), respectively, the activity was diminished to 5 and 3-fold, respectively. In contrast to our observation in propanamide series, where the 4-methoxyphenyl ring on the amino acid was more effective compared to the 4-fluorophenyl ring (**11** vs **9**), comparison in the butanamide series revealed that compounds with 4-fluorophenyl ring was relatively more active compared to its 4-methoxyphenyl counterpart (**2** (IC$_{50}$ = 2.4 μM) vs **5** (IC$_{50}$ = 3.1 μM)). This suggested that electronegative fluoro or methoxy groups attached to C-4 of phenyl ring of amino acid may play an important role in the interaction with the active site of enzyme. All target compounds **2**–**16** were also tested for *in vitro* inhibition against recombinant purified FT enzyme, using inhibitor FT-277 as control. The screening results, summarized in Table 1, revealed that compounds **2**–**16** do not show any activity at 100 μM concentration which suggested that these compounds are selective inhibitors of GGT1.

Scheme 5. Synthesis of **13**–**16**.

Table 1
In vitro GGT1 and FT activity, impact on GTPase Rap1A and MTT assay of compounds **2**–**16**.

Compd	GGT1 (IC$_{50}$, µM)[a]	FT (IC$_{50}$, µM)[a]	Rap1A[c]	MTT Assay (IC$_{50}$, µM)[d]
1 (DU40)	3.3	1.1[b]	+++++	23.0 ± 1.22
2	2.4	> 100	+++++	7.6 ± 1.08
3	11.6	> 100	++	29.4 ± 1.01
4	7.8	> 100	+++	> 50
5	3.1	> 100	+++++	33.2 ± 1.29
6	22.9	> 100	+	15.4 ± 1.03
7	31.9	> 100	++	> 50
8	26.3	> 100	+++	13.2 ± 1.06
9	19.7	> 100	++	> 50
10	34.8	> 100	+	14.8 ± 1.08
11	9.9	> 100	++	> 50
12	> 50	> 100	−	> 50
13	> 50	> 100	−	> 50
14	> 50	> 100	−	> 50
15	26.9	> 100	−	34.9 ± 1.06
16	19.0	> 100	−	26.5 ± 1.10

[a] Each measurement was performed as triplicate.
[b] Inhibitor FTI-277 as control.
[c] Impact on GTPase Rap1A in cells (5 µM, 48 h).
[d] Assay in MDA-MB-231 cells, repeated 3 times (individual experiments) with 2 different time points of 48 h and 72 h. Data presented by one set of experiment with one time point (72 h). + represents fold difference after normalization with internal control tubulin.

2.2.2. Western blot analysis

Rap1A is normally isoprenylated by GGT1 and is used as an indicator for protein geranylgeranylation. In the Western blot analysis, the impairment of prenylation is noted by the use of anti-Rap1A antibody that selectively recognizes the unprenylated form of the Rap1A, a band indicating an alteration in Rap1A geranylgeranylation. This cellular assay was used to examine the capacity of the compounds to inhibit GGT1 in an intact cell, namely the breast cancer cell line MDA-MB-231. ImageJ software was used to quantitate the Rap1A expression and normalized with internal control tubulin (Table 1). In normal growing cells treated with the DMSO control (10 µl of DMSO (0.5%)), all the Rap1A was geranylgeranylated and the band was fairly blank. When GGT1 was inhibited by GGTI-DU40 (control), the accumulation of unprenylated Rap1A was readily observed (Fig. 2). Compounds **2** and **5** have
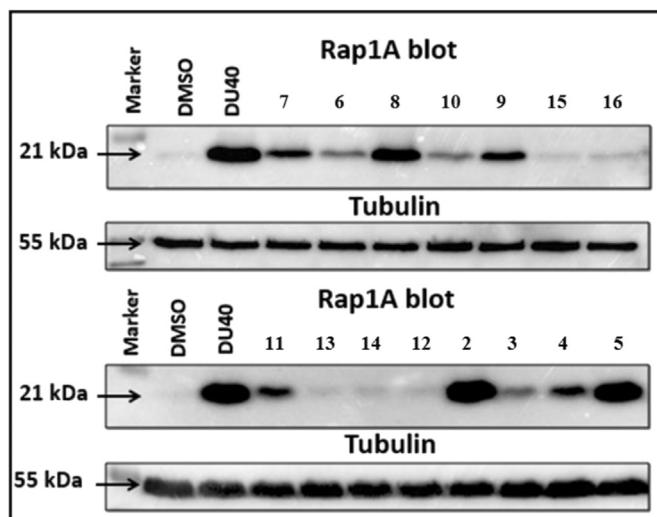
Fig. 2. Inhibition of geranylgeranylation of Rap1A in MDA-MB-231 cells by **2**–**16**. Western blots of Rap1A following 48-h treatment with the indicated inhibitors at a concentration of 5 µM. Tubulin was used as the loading control for the immunoblot and GGTI-DU40 as the positive control inhibitor. The anti-Rap1A antibody detects the unprenylated form of Rap1A, a band indicating a reduction in Rap1A geranylgeranylation.

shown the highest level of Rap1A expression, which is in line with their highest GGT1 inhibitory activity. These data indicate the capacity of **2** and **5** to inhibit prenylation of endogenous proteins. Moreover, compounds with comparable GGT1 inhibitory activity have shown almost similar alteration in Rap1A geranylgeranylation. For instance, compounds **4** (IC$_{50}$ = 7.8 μM) and **11** (IC$_{50}$ = 9.9 μM) have exhibited similar levels of Rap1A expression as well as compounds **6** (IC$_{50}$ = 22.9 μM) and **10** (IC$_{50}$ = 34.8 μM). Likewise, compounds **12**–**14** that were inactive in the GGT1 inhibition did not alter Rap1A geranylgeranylation. The lower cellular activities of compounds **3**, **15** and **16** suggest that they may be less capable of permeating the cells (Fig. 2).

2.2.3. Cell proliferation assay

To determine the *in vitro* dose-dependent cytotoxicity effect of compounds **2**–**16**, the potency of **2**–**16** to inhibit growth of breast cancer cells MDA-MB-231 were assessed using the MTT assay. This colorimetric assay is based on the ability of mitochondrial enzymes of live cells to reduce MTT to formazan salt. The cultured cells were treated with compounds at various concentrations (2–32 μM) followed by measuring cell growth using the CellTiter 96® Aqueous one (Promega) cell proliferation assay solution after 48 h. The cytotoxic effects of the extracts were then estimated in terms of growth inhibition percentage with reference to the control (DMSO treated cells) and expressed as IC$_{50}$ values (Table 1). Whereas compounds **12**–**14** were found to be inactive in both GGT1 inhibition and MTT assays, the activities of compounds **6**, **8**, **15** and **16** were almost comparable i.e. showing moderate GGT1 inhibition and cytotoxicity in the MTT assay. In addition, **2** (IC$_{50}$ = 7.6 μM) turned out to be the most active compound, which showed significantly higher activity compared to **1** (IC$_{50}$ = 23.0 μM). There is a general, but not perfect, correlation with impact on Rap1A prenylation and IC$_{50}$ in the MTT assay, both of which read out cellular activity. The GGT1 IC$_{50}$ may not correlate for reasons of cell permeability as noted above.

2.3. Molecular docking studies

In order to examine the possible binding mode of **2**–**16**, compound **2** was docked into the GGT1 binding pocket based on the co-crystal structure of GGT1 complexed with a GGPP Analog and a KKKSKTKCVIL peptide (PDB ID: 1N4Q) using Glide (Glide, Schrodinger Inc.) [40]. The GGT1 binding pocket is lined by mainly hydrophobic residues that bind the methyl-5-geranyl-4-methyl-pent-3-enyl moiety. At the entrance of the binding pocket, the positively charged residues Arg172, Lys266, Arg263, and His219 bind to the phosphate group of the co-crystallized ligand (Figure S-1). Computationally removing the KKKSKTKCVIL peptide substrate from the enzyme, exposed a large volume of the active site, which in turn resulted in different docking poses of **2** using the two scoring functions of Glide, SP and XP [41,42]. Based on Fig. 3a and b, Thr45 and Arg173 serve as hydrogen bond donors for the primary amide oxygen and oxygen at C-5 of the pyrazole moiety, respectively. Similarly, Ser46 and Thr49 are hydrogen bond acceptors for the primary amide hydrogens of **2** (Fig. 3b). In addition, **2** is engaged in π-π contacts through the 4-fluorophenyl (Fig. 3a) and ,4-dichlorophenyl moieties (Fig. 3b) to the imidazole moiety of His121 and via pyridyl ring to the phenyl moiety of Tyr126 (Fig. 3b). However, when the KKKSKTKCVIL peptide was kept in the binding pocket, the obtained poses using the SP and XP scoring functions of Glide are very similar. The central pyrimidine phenyl diazole is kept inside the hydrophobic pocket, while the peptidic part orients itself towards the solvent and assumes different conformations between the SP and XP modes. By keeping the KKKSKTKCVIL peptide in the pocket, Glu169 and Leu511 acted as hydrogen bond acceptors for

the primary amide hydrogens of **2** (Fig. 3c) as well as for Asp269 (Fig. 3d). Additional hydrogen bond interactions were evident between the nitrogen (N-2) of the pyrazole moiety of **2** with Gln212 (Fig. 3c and d) as well as between the Arg263 and Tyr272 with the secondary and primary amide oxygens, respectively (Fig. 3d). Additional π-π contacts of **2** were observed through the 3,4-dichlorophenyl, pyridyl, pyrazole and 4-fluorophenyl moieties with Hie219, Trp272, Arg263 and Lys311 (Fig. 3c and d).

3. Experimental

3.1. Chemistry

General: Melting points were determined on a Büchi apparatus (Büchi Labortechnik AG, Switzerland) and are uncorrected. Elemental analysis was carried out on a Perkin Elmer Elemental Analyzer Series 11 Model 2400 (PerkinElmer Inc. USA). IR spectra were recorded on a Perkin Elmer 16F PC FTIR spectrophotometer (PerkinElmer Inc. USA). ^{1}H and ^{13}C NMR spectra were measured in CDCl$_3$ and DMSO-d_6 using TMS as internal standard on a JEOL JNM-LA 500 MHz spectrometer (JEOL USA Inc.). Analytical TLC was carried out on silica gel 60 F$_{254}$ plates (E. Merck); column chromatography was carried out on silica gel (200–400 mesh, E. Merck).

3.2. Synthetic procedures for the intermediates and target compounds

#### 3.2.1. (S)-2-amino-3-(4-fluorophenyl)propanamide (25)

In a pressure vessel, a solution of compound **20** [28] (0.50 g, 2.54 mmol) in NH$_4$OH (2 mL) was heated overnight at 100 °C. After cooling to room temperature, CH$_2$Cl$_2$ (10 mL) was added in the reaction mixture and the organic layer was separated and dried over Na$_2$SO$_4$ and evaporated to get the title compound **25** as a light yellow solid (yield 95%). M. p. 153–154 °C. IR (neat): 3377, 3329, 2958, 2926, 2834, 1667, 1613, 1512, 1448, 1299, 1249, 1035 cm^{-1}; ^{1}H NMR (500 MHz, CD$_3$OD): δ 3.04 (dd, *J* = 7.65, 13.9 Hz, 1H, *CH$_2$*CH), 3.20 (dd, *J* = 5.8, 13.9 Hz, 1H, *CH$_2$*CH), 4.06 (m, 1H, CH$_2$*CH*), 7.08 (m, 2H, 3'-H, 5'-H), 7.31 (m, 2H, 2'-H, 6'-H); ^{13}C NMR (125.7 MHz, CD$_3$OD): δ 37.82 (*CH$_2$*CH), 55.60 (CH$_2$*CH*), 116.76 (d, *J* = 21.8 Hz, C-3', C-5'), 132.40 (d, *J* = 8.3 Hz, C-2', C-6'), 134.40 (C-1') 163.70 (d, *J* = 247.0 Hz, C-4'), 171.82 (C═O). Anal. Calcd for C$_9$H$_{11}$FN$_2$O (198.19): C 59.33 H 6.09, N 15.38. Found: C 59.29, H 6.13, N 15.31.

3.2.2. (S)-2-amino-3-(pyridin-3-yl)propanamide (26)

Following the procedure adopted for the synthesis of **25**, the reaction of **21** [29] with NH$_4$OH yielded compound **26** as a light yellow solid (yield 88%). M. p. 114–115 °C. IR (neat): 3366, 2977, 2936, 1703, 1519, 1429, 1346, 1168, 1036 cm^{-1}; ^{1}H NMR (500 MHz, CD$_3$OD): δ 2.88 (dd, *J* = 7.3, 13.7 Hz, 1H, *CH$_2$*CH), 3.04 (dd, *J* = 6.4, 13.7 Hz, 1H, *CH$_2$*CH), 3.62 (t, *J* = 7.0 Hz, 1H, CH$_2$*CH*), 7.37 (m, 1H, 5'-H), 7.75 (m, 1H, 6'-H), 8.40 (d, *J* = 6.5 Hz, 1H, 4'-H), 8.42 (d, *J* = 1.3 Hz, 1H, 2'-H); ^{13}C NMR (125.7 MHz, CD$_3$OD): δ 34.85 (*CH$_2$*CH), 54.48 (CH$_2$*CH*), 125.22, 131.34, 139.39, 148.59, 149.70 (all C$_{arom}$), 172.23 (C═O). Anal. Calcd for C$_8$H$_{11}$N$_3$O (181.19): C 58.17, H 6.71, N 25.44. Found: C 58.13, H 6.76, N 25.37.

3.2.3. (S)-2-amino-3-(pyridin-4-yl)propanamide (27)

Following the procedure adopted for the synthesis of **25**, the reaction of compound **22** with NH$_4$OH gave compound **27** as a light yellow solid (yield 85%). M. p. 158–159 °C. IR (neat): 3364, 3250, 3035, 2939, 1695, 1607, 1539, 1420, 1398, 1038 cm^{-1}; ^{1}H NMR (500 MHz, CD$_3$OD): δ 3.05 (dd, *J* = 7.9, 14.0 Hz, 1H, *CH$_2$*CH), 3.22 (dd, *J* = 5.4, 14.0 Hz, 1H, *CH$_2$*CH), 4.02 (m, 1H, CH$_2$*CH*), 7.38 (d, *J* = 6.1 Hz, 2H, 2'-H, 6'-H), 8.50 (d, *J* = 6.1 Hz, 2H, 3'-H, 5'-H); ^{13}C NMR (125.7 MHz, CD$_3$OD): δ 37.50 (*CH$_2$*CH), 56.48 (CH$_2$*CH*), 126.53 (C-2',
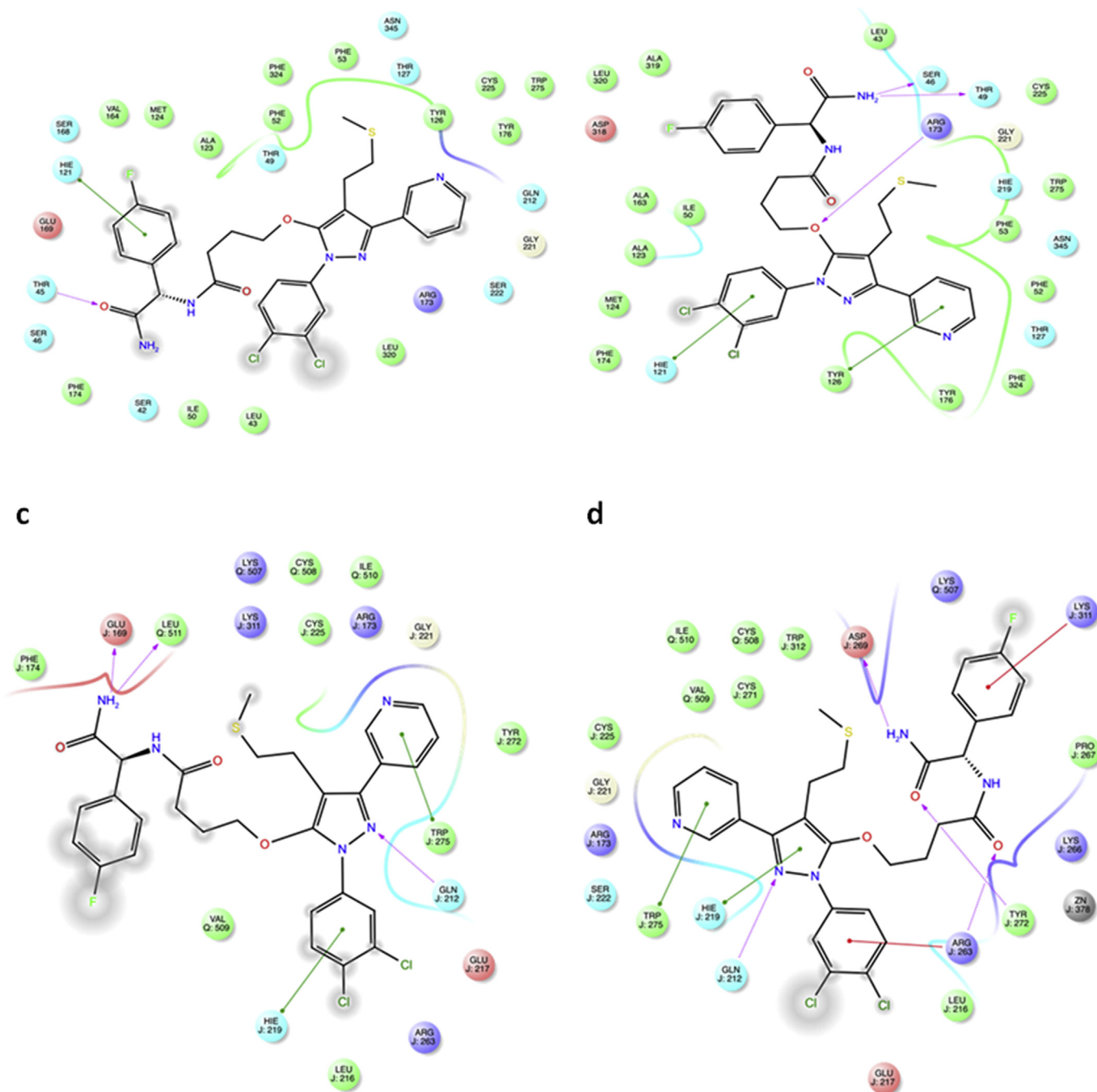
Fig. 3. Molecular docking of **2** into the GGT1 binding pocket without the KKKSKTKCVIL peptide (a) using the Glide SP mode and (b) using the Glide XP mode. Molecular docking of **2** into the GGT1 binding pocket in presence of the KKKSKTKCVIL peptide (c) using the Glide SP mode and (d) using the Glide XP mode.

C-6′), 146.97 (C-1′), 150.47 (C-3′, C-5′), 172.60 (C=O). Anal. Calcd for $C_8H_{11}N_3O_2$ (181.19): C 58.17, H 6.71, N 25.44. Found: C 58.14, H 6.75, N 25.37.

3.2.4. (S)-2-amino-3-(4-methoxyphenyl)propanamide (28)

Following the procedure adopted for the synthesis of **25**, the reaction of compound **24** [32] with NH_4OH gave the title compound **28** [35] as a light yellow solid (yield 94%). M. p. 177−178 °C. IR (neat): 3376, 3056, 2958, 1667, 1613, 1511, 1449, 1299, 1250, 1035 cm^{-1}; ^{1}H NMR (500 MHz, CD$_3$OD): δ 2.75 (dd, J = 7.6, 13.9 Hz, 1H, CH$_2$), 2.91 (dd, J = 6.1, 13.9 Hz, 1H, CH$_2$), 3.53 (m, 1H, CH), 3.75 (s, 3H, OCH$_3$), 6.85 (d, J = 8.5 Hz, 2H, 3′-H, 5′-H), 7.15 (d, J = 8.3 Hz, 2H,

2′-H, 6′-H); ^{13}C NMR (125.7 MHz, CD$_3$OD): δ 41.42 (CH$_2$CH), 55.65 (OCH$_3$), 57.37 (CH$_2$CH), 114.17 (C-3′, C-5′), 130.51 (C-1′), 131.41 (C-2′, C-6′), 160.12 (C-4′), 179.19 (C=O). Anal. Calcd for $C_{10}H_{14}N_2O_2$ (210.23): C 61.84, H 7.27, N 14.42. Found: C 61.79, H 7.33, N, 14.35.

3.2.5. 2-(1-(3,4-Dichlorophenyl)-5-hydroxy-3-(pyridin-3-yl)-1H-pyrazol-4-yl)ethyl acetate (47)

A slightly modified procedure was followed [38]. 3,4-Dichlorophenylhydrazine hydrochloride (5.86 g, 27.5 mmol) was added to the solution of α-ketobutyrolactone **46** (4.78 g, 25.03 mmol) in acetic acid (20 mL) in one portion. The mixture was heated at reflux overnight and then cooled to room temperature.

The mixture was diluted with H_2O (20 mL) and then extracted with EtOAc (2 × 30 mL). The combined organic layers was washed with sat. aqueous $NaHCO_3$ (2 × 15 mL), dried over Na_2SO_4 and evaporated under reduced pressure. Column chromatography of the light oily material eluting with EtOAc-hexane (1:1) afforded the title compound **47** as a yellow solid (8.22 g, 84%). M. p. 176−177 °C. IR (neat): 3426, 3099, 3076, 2993, 2984, 1725, 1589, 1475, 1409, 1250, 1025 cm^{-1}; ^{1}H NMR (500 MHz, DMSO-d_6): δ 1.78 (s, 3H, COCH_3), 2.84 (t, J = 6.4 Hz, 2H, ArCH_2), 4.03 (t, J = 6.5 Hz, 2H, OCH_2), 7.49 (dd, J = 2.1, 8.7 Hz, 1H, Ar-H), 7.73 (d, J = 8.8 Hz, 1H, Ar-H), 7.84 (dd, J = 2.1, 6.8 Hz, 1H, Ar-H), 8.06 (m, 2H, Ar-H), 8.58 (d, J = 1.8 Hz, 1H, Ar-H), 8.86 (s, 1H, Ar-H); ^{13}C NMR (125.7 MHz, DMSO-d_6): δ 20.55 (COCH_3), 21.63 (Ar-CH_2), 63.13 (OCH_2), 120.65, 122.04, 123.84, 127.87, 131.09, 131.49, 135.01, 138.18, 147.79, 148.01, 149.17 (all C_{arom}), 170.31 (C=O). Anal. Calcd for $C_{18}H_{15}Cl_2N_3O_3$ (391.05): C 55.12, H 3.85, N 10.71%. Found: C 55.08, H 3.89, N 10.65%.

3.2.6. Ethyl 4-((4-(2-acetoxyethyl)-1-(3,4-dichlorophenyl)-3-(pyridin-3-yl)-1H-pyrazol-5-yl)oxy)buta-noate (48)

K_2CO_3 (1.06 g, 7.65 mmol) was added to a solution of **47** (2.0 g, 5.10 mmol) in anhydrous DMF (20 mL) followed by the addition of ethyl 4-bromobutanoate (0.88 mL, 6.12 mmol). The mixture was stirred for 4 h at room temperature until the completion of the reaction (TLC analysis). The reaction was diluted with EtOAc (30 mL) and then washed successively with 1 M aqueous HCl (10 mL), H_2O (10 mL) and brine (10 mL). The organic layer was dried over anhydrous Na_2SO_4 and evaporated under reduced pressure. Column chromatography of the light orange oily material, eluting with EtOAc-hexane (8:2) afforded the title compound **48** as a yellow thick oil (1.42 g, 54%). IR (neat): 3034, 2954, 1740, 1592, 1484, 1415, 1366, 1230, 1029 cm^{-1}; ^{1}H NMR (500 MHz, CD$_3$OD): δ 1.26 (t, J = 7.0 Hz, 2H, CH_3CH$_2$O), 1.96 (s, 3H, COCH_3), 2.07 (quint, 2H, J = 6.7 Hz, 2H, -CH$_2$$CH_2CH_2$-), 2.48 (t, J = 7.3 Hz, 2H, CH_2CO$_2$Et), 2.96 (t, J = 7.0 Hz, 2H, ArCH_2), 4.04 (t, J = 6.4 Hz, 2H, OCH_2), 4.14 (q, J = 7.0 Hz, 2H, CH$_3$$CH_2$O), 4.19 (t, J = 7.0 Hz, 2H, OCH_2), 7.57 (d, J = 8.8 Hz, 1H, Ar-H), 7.61−7.66 (m, 2H, Ar-H), 7.93 (d, J = 2.4 Hz, 1H, Ar-H), 8.36 (d, J = 7.9 Hz, 1H, Ar-H), 8.67 (d, J = 4.5 Hz, 1H, Ar-H), 9.06 (br. s, 1H, Ar-H); ^{13}C NMR (125.7 MHz, CD$_3$OD): δ 14.16 (CH_3CH$_2$O), 20.08 (COCH_3), 22.41 (Ar-CH_2), 25.03 (-CH$_2$$CH_2CH_2$-), 30.17 ($CH_2CO_2$Et), 60.68 (CH$_3$$CH_2$O), 63.30 (O$CH_2$), 74.67 (O$CH_2$), 103.13, 121.05, 123.83, 124.79, 130.65, 130.89, 131.25, 133.32, 137.30, 137.98, 144.95, 145.36, 146.39, 152.43 (all C_{arom}), 170.83 (C=O), 172.44 (C=O). Anal. Calcd for $C_{24}H_{25}Cl_2N_3O_5$ (505.12): C 56.93, H 4.98, N 8.30%. Found: C 56.85, H 5.03, N 8.25%.

3.2.7. 4-((1-(3,4-Dichlorophenyl)-4-(2-hydroxyethyl)-3-(pyridin-3-yl)-1H-pyrazol-5-yl)oxy)butanoic acid (49)

LiOH.H_2O (0.68 g, 16.2 mmol) was added to a solution of **48** (1.64 g, 3.24 mmol) in a mixture of MeOH-H_2O-THF (25 mL, 1:1:3), and the mixture was stirred for 4 h at room temperature until the completion of the reaction (TLC analysis). The volatiles were evaporated under reduced pressure to get the title compound **49** as a white crystalline solid (1.10 g, 78%). M. p. 119-120 °C. IR (neat): 3388, 2954, 2922, 1677, 1594, 1489, 1452, 1368, 1146, 1024 cm^{-1}; ^{1}H NMR (500 MHz, CD$_3$OD): δ 2.00 (quint, J = 7.3 Hz, 2H, -CH$_2$$CH_2CH_2$-), 2.28 (t, J = 7.3 Hz, 2H, CH_2CO$_2$H), 2.86 (t, J = 7.3 Hz, 2H, ArCH_2), 3.66 (t, J = 7.0 Hz, 2H, OCH_2), 4.08 (t, J = 6.7 Hz, 2H, OCH_2), 7.53 (dd, J = 4.8, 7.9 Hz, 1H, Ar-H), 7.68 (d, J = 8.5 Hz, 1H, Ar-H), 7.75 (dd, J = 2.4, 8.8 Hz, 1H, Ar-H), 7.97 (d, J = 2.4 Hz, 1H, Ar-H), 8.18 (m, 1H, Ar-H), 8.55 (dd, J = 1.5, 4.8 Hz, 1H, Ar-H), 8.89 (d, J = 1.4 Hz, 1H, Ar-H); ^{13}C-NMR (125.7 MHz, CD$_3$OD): δ 26.36 (ArCH_2), 27.22 (-CH$_2$$CH_2CH_2$-), 31.22 ($CH_2CO_2$H), 62.19 (O$CH_2$), 75.86 (O$CH_2$), 105.20, 123.06, 125.26, 131.71, 131.91, 132.26, 134.01, 137.33, 139.17, 149.08, 149.55, 153.89 (all C_{arom}), 176.75 (C=O). Anal. Calcd for $C_{20}H_{19}Cl_2N_3O_4$ (435.08): C 55.06, H 4.39, N 9.63%. Found: C 55.0, H 4.45, N 9.55%.

3.2.8. (S)-N-(1-Amino-3-(4-fluorophenyl)-1-oxopropan-2-yl)-4-((1-(3,4-dichlorophenyl)-4-(2-hydroxyethyl)-3-(pyridin-3-yl)-1H-pyrazol-5-yl)oxy)butanamide (50)

Hydroxybenzotriazole (0.17 g, 1.1 mmol), N-(3-dimethylaminopropyl)-N′-ethylcarbodiimide hydrochloride (0.28 g, 1.46 mmol) and Et$_3$N (0.51 mL, 3.65 mmol) was sequentially added to a solution mixture of compound **25** (0.089 g, 0.49 mmol) and **49** (0.32 g, 0.73 mmol) in anhydrous CH$_2$Cl$_2$ (15 mL), and the reaction was stirred overnight at room temperature. The mixture was diluted with ethyl acetate (30 mL) and washed with H_2O (10 mL) and brine (10 mL). The organic layer was dried over Na$_2$SO$_4$ and evaporated under reduced pressure. Column chromatography of thick oily material, eluting with the EtOAc-hexane (8:2), gave the desired product **50** as a white solid (yield 68%). M. p. 182−183 °C. IR (neat): 3356, 3292, 3051, 2956, 1632, 1593, 1481, 1418, 1222, 1028 cm^{-1}; ^{1}H NMR (500 MHz, CD$_3$OD): δ 1.92 (t, J = 6.7 Hz, 2H, COCH_2), 2.30 (pent, 2H, CH$_2$$CH_2CH_2$), 2.83 (m, 3H, Ar$CH_2$, CH_2CH), 3.12 (dd, J = 4.9, 11.6 Hz, 1H, CH_2CH), 3.66 (t, J = 7.0 Hz, 2H, OCH_2), 3.96 (t, J = 6.7 Hz, 2H, OCH_2), 4.58 (m, 1H, CH$_2$$CH$), 6.93 (m, 2H, Ar-H), 7.21 (m, 2H, Ar-H), 7.53 (dd, J = 2.4, 8.1 Hz, 1H, Ar-H), 7.65−7.71 (m, 2H, Ar-H), 7.93 (d, J = 2.1 Hz, 1H, Ar-H), 8.17 (dd, J = 2.3, 8.1 Hz, 1H, Ar-H), 8.55 (d, J = 8.3 Hz, 1H, Ar-H), 8.88 (d, J = 2.3 Hz, 1H, Ar-H); ^{13}C NMR (125.7 MHz, CD$_3$OD): δ 26.81 (ArCH_2), 27.21 (CH$_2$$CH_2CH_2$), 32.77 (CO$CH_2$), 38.26 ($CH_2$CH), 55.52 (O$CH_2$), 62.21 (CH$_2$$CH$), 75.81 (O$CH_2$), 105.19, 115.98 (d, J = 21.8 Hz), 122.94, 125.13, 125.27, 131.70, 131.81, 131.95, 132.27, 133.97, 134.57, 137.32, 139.18, 149.05, 149.56, 153.81, 163.56 (d, J = 248.0 Hz) (all C_{arom}), 174.65 (C=O), 176.05 (C=O). Anal. Calcd for $C_{29}H_{28}Cl_2FN_5O_4$ (600.47): C 58.01, H 4.70, N 11.66%. Found: C 57.94, H 4.76, N 11.60%.

3.2.9. (S)-N-(1-amino-1-oxo-3-(pyridin-3-yl)propan-2-yl)-4-((1-(3,4-dichlorophenyl)-4-(2-hydroxyethyl)-3-(pyridin-3-yl)-1H-pyrazol-5-yl)oxy)butanamide (51)

Following the procedure adopted for the synthesis of **50**, the reaction of **49** with **26** gave compound **51** as a yellowish gum (yield 62%). IR (neat): 3417, 2925, 1668, 1593, 1482, 1368, 1024 cm^{-1}; ^{1}H NMR (500 MHz, CD$_3$OD): δ 1.90 (t, J = 6.7 Hz, 2H, COCH_2), 2.31 (pent, 2H, CH$_2$$CH_2CH_2$), 2.83 (t, J = 6.7 Hz, 2H, ArCH_2), 2.89 (dd, J = 9.1, 13.7 Hz, 1H, CH_2CH), 3.19 (dd, J = 5.5, 13.7 Hz, 1H, CH_2CH), 3.65 (t, J = 7 Hz, 2H, OCH_2), 3.95 (t, J = 6.7 Hz, 2H, OCH_2), 4.60 (m, 1H, CH$_2$$CH$), 7.31 (dd, J = 4.8, 8.5 Hz, 1H, Ar-H), 7.53 (dd, J = 4.9, 8.2 Hz, 1H, Ar-H), 7.67 (d, J = 8.7 Hz, 1H, Ar-H), 7.70 (dd, J = 2.45 Hz, 1H, Ar-H), 7.73 (m, 1H, Ar-H), 7.94 (d, J = 2.4 Hz, 1H, Ar-H), 8.20 (dd, J = 2.15, 8.0 Hz, 1H, Ar-H), 8.33 (dd, J = 1.5, 4.9 Hz, 1H, Ar-H), 8.41 (d, J = 1.5 Hz, 1H, Ar-H), 8.56 (dd, J = 1.5, 4.9 Hz, 1H, Ar-H), 8.89 (d, J = 1.5 Hz, 1H, Ar-H); ^{13}C NMR (125.7 MHz, CD$_3$OD): δ 26.79 (ArCH_2), 27.23 (CH$_2$$CH_2CH_2$), 32.73 (CO$CH_2$), 36.23 ($CH_2$CH), 54.89 (O$CH_2$), 62.19 (CH$_2$$CH$), 75.84 (O$CH_2$), 105.25, 122.92, 125.08, 125.11, 125.29, 131.68, 131.80, 132.28, 133.97, 135.29, 137.32, 139.06, 139.17, 148.34, 149.03, 149.47, 149.57, 150.79, 153.82 (all C_{arom}), 174.67 (C=O), 175.51 (C=O). Anal. Calcd for $C_{28}H_{28}Cl_2N_6O_4$ (543.47): C 57.64, H 4.84, N 14.40. Found: C 57.57, H 4.89, N 14.33.

3.2.10. (S)-N-(1-amino-1-oxo-3-(pyridin-4-yl)propan-2-yl)-4-((1-(3,4-dichlorophenyl)-4-(2-hydroxy-ethyl)-3-(pyridin-3-yl)-1H-pyrazol-5-yl)oxy)butanamide (52)

Following the procedure adopted for the synthesis of **50**, the reaction of **49** with **27** gave compound **52** as a white solid (yield 60%). M. p. 159−160 °C. IR (neat): 3402, 2924, 1689, 1592, 1482, 1367, 1134, 1029 cm^{-1}; ^{1}H NMR (500 MHz, CD$_3$OD): δ 1.91 (t, J = 6.7 Hz, 2H, COCH_2), 2.32 (pent, 2H, CH$_2$$CH_2CH_2$), 2.83 (t, J = 6.7 Hz, 2H, ArCH_2), 2.91 (dd, J = 9.7, 13.7 Hz, 1H, CH_2CH), 3.20 (dd, J = 5.5, 13.7 Hz, 1H, CH_2CH), 3.64 (t, J = 7 Hz, 2H, OCH_2), 3.97 (t,

$J = 6.4$ Hz, 2H, OCH_2), 4.71 (m, 1H, CH$_2$CH), 7.32 (d, $J = 6.1$ Hz, 2H, Ar-H), 7.54 (m, 1H, Ar-H), 7.67 (d, $J = 8.8$ Hz, 1H, Ar-H), 7.71 (d, $J = 8.8$ Hz, 1H, Ar-H), 7.94 (d, $J = 2.4$ Hz, 1H, Ar-H), 8.19 (d, $J = 8.5$ Hz, 1H, Ar-H), 8.40 (dd, $J = 1.5, 4.9$ Hz, 1H, Ar-H), 8.56 (dd, $J = 1.7, 4.9$ Hz, 1H, Ar-H), 8.89 (d, $J = 1.5$ Hz, 1H, Ar-H); ^{13}C NMR (125.7 MHz, CD$_3$OD): δ 26.81 (ArCH_2), 27.23 (CH$_2$$CH_2CH_2$), 32.74 (CO$CH_2$), 38.34 ($CH_2$CH), 54.37 (OC$H_2$), 62.21 (CH$_2$$CH$), 75.86 (OC$H_2$), 105.22, 125.96, 125.14, 125.29, 126.34, 131.70, 131.81, 132.27, 133.97, 137.32, 139.18, 149.04, 149.49, 149.57, 149.92, 153.82 (all C$_{arom}$), 174.74 (C=O), 175.43 (C=O). Anal. Calcd for C$_{28}$H$_{28}$Cl$_2$N$_6$O$_4$ (583.47): C 57.64, H 4.84, N 14.40. Found: C 57.56, H 4.88, N 14.33.

3.2.11. (S)-N-(1-amino-3-(4-methoxyphenyl)-1-oxopropan-2-yl)-4-((1-(3,4-dichlorophenyl)-4-(2-hydroxyethyl)-3-(pyridin-3-yl)-1H-pyrazol-5-yl)oxy)butanamide (53)

Following the procedure adopted for the synthesis of **50**, the reaction of **49** with **28** gave compound **53** as a white solid (yield 66%). M. p. 175–176 °C. IR (neat): 3350, 3274, 3189, 2925, 1676, 1641, 1593, 1482, 1248, 1049 cm^{-1}; ^{1}H NMR (500 MHz, CD$_3$OD): δ 1.91 (t, $J = 6.7$ Hz, 2H, COCH_2), 2.30 (pent, 2H, CH$_2$CH_2CH$_2$), 2.75 (dd, $J = 9.1$, 13.7 Hz, 1H, CH_2CH), 2.82 (t, $J = 6.7$ Hz, 2H, ArCH_2), 3.06 (dd, $J = 5.5$, 13.7 Hz, 1H, CH_2CH), 3.64 (t, $J = 7.3$ Hz, 2H, OCH_2), 3.97 (t, $J = 7.0$ Hz, 2H, OCH_2), 4.58 (m, 1H, CH$_2$CH), 6.76 (d, $J = 8.5$ Hz, 2H, Ar-H), 7.14 (d, $J = 8.5$ Hz, 2H, Ar-H), 7.53 (m, 1H, Ar-H), 7.65 (d, $J = 8.8$ Hz, 1H, Ar-H), 7.69 (dd, $J = 2.1, 8.5$ Hz, 1H, Ar-H), 7.94 (d, $J = 2.1$ Hz, 1H, Ar-H), 8.56 (dd, $J = 1.7, 4.9$ Hz, 1H, Ar-H), 8.89 (d, $J = 1.5$ Hz, 1H, Ar-H); ^{13}C NMR (125.7 MHz, CD$_3$OD): δ 26.83 (ArCH_2), 27.25 (CH$_2$$CH_2CH_2$), 32.70 (CO$CH_2$), 38.30 ($CH_2$CH), 54.39 (OC$H_2$), 62.20 (CH$_2$$CH$), 75.82 (OC$H_2$), 107.12, 115.22, 115.75, 122.39, 124.92, 125.07, 129.47, 131.24, 131.26, 131.65, 132.27, 134.58, 136.36, 139.09, 149.31, 149.85, 150.70, 153.44, 159.10 (all C$_{arom}$), 172.80 (C=O), 174.30 (C=O). Anal. Calcd for C$_{30}$H$_{31}$Cl$_2$N$_5$O$_5$ (612.50): C 58.83, H 5.10, N 11.43. Found: C 58.77, H 5.16, N 11.35.

3.2.12. (S)-N-(1-amino-3-(4-fluorophenyl)-1-oxopropan-2-yl)-4-((1-(3,4-dichlorophenyl)-4-(2-(methylthio)ethyl)-3-(pyridin-3-yl)-1H-pyrazol-5-yl)oxy)butanamide (2)

Et$_3$N (0.1 mL, 0.75 mmol) was added to a solution of compound **50** (0.15 g, 0.25 mmol) in THF (5 mL) at 0 °C and after being stirred for 10 min, a solution of MsCl (0.03 mL, 0.37 mmol) in THF (1 mL) was added dropwise. The reaction mixture was stirred for 2 h and was then diluted with ethyl acetate (15 mL) and successively washed with H$_2$O (5 mL) and brine (2 × 5 mL). The organic layer was dried over Na$_2$SO$_4$ and evaporated under reduced pressure to get the mesylated product as light yellow thick oil, which was dissolved in DMF (7 mL) followed by the addition of sodium methane thiolate (0.04 g, 0.5 mmol) at 0 °C. The stirring continued for 2 h until the completion of the reaction (TLC analysis) and the mixture was then diluted with ethyl acetate (15 mL) and successively washed with H$_2$O (5 mL) and brine (2 × 5 mL). The organic layer was dried over Na$_2$SO$_4$ and evaporated under reduced pressure. Column chromatography of the light yellow oily material eluting with EtOAc-hexane (8:2) gave the title compound **2** as a colorless solid (yield 85%). M. p. 140–141 °C. IR (neat): 3398, 3309, 3205, 3072, 2919, 1661, 1592, 1482, 1366, 1221, 1025 cm^{-1}; ^{1}H NMR (500 MHz, CDCl$_3$): δ 2.03–2.08 (m, 5H, SCH$_3$, COCH_2), 2.36 (pent, 2H, CH$_2$CH_2CH$_2$), 2.63 (t, $J = 7.6$ Hz, 2H, SCH_2), 2.87 (t, $J = 7.5$ Hz, 2H, ArCH_2), 3.03 (m, 2H, CH_2CH), 3.99 (t, $J = 7.1$ Hz, 2H, OCH_2), 4.62 (m, 1H, CH$_2$CH), 6.25 (d, $J = 7.3$ Hz, 1H, NH), 6.97 (m, 2H, Ar-H), 7.21 (m, 2H, Ar-H), 7.39 (m, 1H, Ar-H), 7.54 (d, $J = 8.8$ Hz, 1H, Ar-H), 7.65 (dd, $J = 2.4, 8.8$ Hz, 1H, Ar-H), 7.93 (d, $J = 2.4$ Hz, 1H, Ar-H), 8.00 (dd, $J = 2.3, 8.5$ Hz, 1H, Ar-H), 8.63 (d, $J = 2.4$ Hz, 1H, Ar-H), 8.89 (s, 1H, Ar-H); ^{13}C NMR (125.7 MHz, CDCl$_3$): δ 15.62 (SCH$_3$), 23.12 (Ar-CH_2), 25.37 (CH$_2$$CH_2CH_2$), 32.11 (CO$CH_2$), 34.04 (S$CH_2$), 37.58 ($CH_2$CH), 54.12 (CH$_2$$CH$), 74.57 (OC$H_2$), 105.74, 115.65 (d, $J = 21.8$ Hz), 115.73,

121.01, 123.63, 130.72, 130.73, 130.76, 130.79, 130.86, 131.98, 132.0 (d, $J = 3.1$ Hz), 133.09, 134.95, 137.65, 148.54, 149.35, 163.59 (d, $J = 247$ Hz) (all C$_{arom}$), 171.42 (C=O), 172.36 (C=O). Anal. Calcd for C$_{30}$H$_{30}$Cl$_2$FN$_5$O$_3$S (630.56): C 57.14, H 4.80, N 11.11. Found C 57.08, H 4.87, N 11.04.

3.2.13. (S)-N-(1-amino-1-oxo-3-(pyridin-3-yl)propan-2-yl)-4-((1-(3,4-dichlorophenyl)-4-(2-(methyl-thio)ethyl)-3-(pyridin-3-yl)-1H-pyrazol-5-yl)oxy)butanamide (3)

Following the procedure adopted for the synthesis of **2**, acylation of **51** with MsCl, followed by condensing the resultant mesylate with sodium methane thiolate, yielded compound **3** as an off white gum (yield 75%). IR (neat): 3393, 3186, 3047, 2958, 2857, 1738, 1673, 1592, 1481, 1366, 1026 cm^{-1}; ^{1}H NMR (500 MHz, CDCl$_3$): δ 1.92 (t, $J = 6.7$ Hz, 2H, COCH_2), 1.99 (s, 3H, SCH$_3$), 2.32 (pent, 2H, CH$_2$CH_2CH$_2$), 2.55 (t, $J = 7.6$ Hz, 2H, SCH_2), 2.81 (t, $J = 6.7$ Hz, 2H, ArCH_2), 3.12 (dd, $J = 7.6, 14.3$ Hz, 1H, CH_2CH), 3.24 (dd, $J = 5.8$, 14.3 Hz, 1H, CH_2CH), 3.91 (t, $J = 6.1$ Hz, 2H, OCH_2), 4.82 (m, 1H, CH$_2$CH), 7.12 (d, $J = 8.1$ Hz, 1H, NH), 7.36 (m, 1H, Ar-H), 7.44–7.49 (m, 2H, Ar-H), 7.58 (dd, $J = 2.4, 8.8$ Hz, 1H, Ar-H), 7.85 (d, $J = 2.4$ Hz, 1H, Ar-H), 7.88 (m, 1H, Ar-H), 7.99 (m, 1H, Ar-H), 8.45 (d, $J = 5.2$ Hz, 1H, Ar-H), 8.56 (d, $J = 5.2$ Hz, 1H, Ar-H), 8.76 (d, $J = 1.7$ Hz, 1H, Ar-H), 8.87 (d, $J = 1.7$ Hz, 1H, Ar-H); ^{13}C NMR (125.7 MHz, CDCl$_3$): δ 15.64 (SCH$_3$), 23.15 (Ar-CH_2), 25.38 (CH$_2$$CH_2CH_2$), 32.10 (CO$CH_2$), 34.03 (S$CH_2$), 35.43 ($CH_2$CH), 53.68 (CH$_2$$CH$), 74.57 (OC$H_2$), 105.77, 121.10, 123.64, 123.60, 129.60, 130.72, 130.88, 132.04, 133.10, 134.96, 136.92, 137.66, 147.92, 148.51, 149.34, 150.40, 151.79 (all C$_{arom}$), 171.60 (C=O), 172.07 (C=O). Anal. Calcd for C$_{29}$H$_{30}$Cl$_2$N$_6$O$_3$S (613.56): C 56.77, H 4.93, N 13.70. Found: C 56.72, H 4.98, N 13.63.

3.2.14. (S)-N-(1-amino-1-oxo-3-(pyridin-4-yl)propan-2-yl)-4-((1-(3,4-dichlorophenyl)-4-(2-(methyl-thio)ethyl)-3-(pyridin-3-yl)-1H-pyrazol-5-yl)oxy)butanamide (4)

Following the procedure adopted for the synthesis of **2**, acylation of **52** with MsCl, followed by condensing the resultant mesylate with sodium methane thiolate, yielded compound **4** as a white solid (yield 67%). M. p. 183–184 °C. IR (neat): 3342, 3279, 3050, 2935, 1681, 1645, 1480, 1420, 1131, 1024 cm^{-1}; ^{1}H NMR (500 MHz, CD$_3$OD): δ 2.0 (t, $J = 6.7$ Hz, 2H, COCH_2), 2.07 (s, 3H, SCH$_3$), 2.38 (pent, 2H, CH$_2$CH_2CH$_2$), 2.63 (t, $J = 7.3$ Hz, 2H, SCH_2), 2.87 (t, $J = 6.7$ Hz, 2H, ArCH_2), 3.10 (dd, $J = 9.3, 13.9$ Hz, 1H, CH_2CH), 3.18 (dd, $J = 5.6, 13.9$ Hz, 1H, CH_2CH), 3.99 (t, $J = 6.7$ Hz, 2H, OCH_2), 4.78 (m, 1H, CH$_2$CH), 7.30 (d, $J = 6.8$ Hz, 2H, Ar-H), 7.41 (m, 1H, Ar-H), 7.55 (d, $J = 8.5$ Hz, 1H, Ar-H), 7.65 (dd, $J = 2.7, 8.5$ Hz, 1H, Ar-H), 7.93 (d, $J = 2.7$ Hz, 1H, Ar-H), 8.03 (m, 1H, Ar-H), 8.53 (d, $J = 6.9$ Hz, 2H, Ar-H), 8.62 (m, 1H, Ar-H), 8.91 (d, $J = 1.7$ Hz, 1H, Ar-H); ^{13}C NMR (125.7 MHz, CDCl$_3$): δ 15.67 (SCH$_3$), 23.17 (Ar-CH_2), 25.39 (CH$_2$$CH_2CH_2$), 32.08 (CO$CH_2$), 34.05 (S$CH_2$), 37.67 ($CH_2$CH), 53.12 (CH$_2$$CH$), 74.61 (OC$H_2$), 105.80, 121.07, 123.66, 123.72, 125.21, 130.92, 135.29, 148.19, 148.29, 148.97, 153.80 (all C$_{arom}$), 171.78 (C=O), 172.07 (C=O). Anal. Calcd for C$_{29}$H$_{30}$Cl$_2$N$_6$O$_3$S (613.56): C 56.77, H 4.93, N 13.70. Found: C 56.73, H 4.98, N 13.64.

3.2.15. (S)-N-(1-amino-3-(4-methoxyphenyl)-1-oxopropan-2-yl)-4-((1-(3,4-dichlorophenyl)-4-(2-(methylthio)ethyl)-3-(pyridin-3-yl)-1H-pyrazol-5-yl)oxy)butanamide (5)

Following the procedure adopted for the synthesis of **2**, acylation of **53** with MsCl, followed by condensing the resultant mesylate with sodium methane thiolate, yielded compound **5** as a colorless solid (yield 70%). M. p. 154–155 °C. IR (neat): 3341, 3300, 3040, 2922, 1677, 1592, 1512, 1481, 1245, 1028 cm^{-1}; ^{1}H NMR (500 MHz, CD$_3$OD): δ 2.05 (t, $J = 7.6$ Hz, 2H, COCH_2), 2.07 (s, 3H, SCH$_3$), 2.36 (pent, 2H, CH$_2$CH_2CH$_2$), 2.63 (t, $J = 7.3$ Hz, 2H, SCH_2), 2.87 (t, $J = 7.6$ Hz, 2H, ArCH_2), 2.99 (dd, $J = 6.1, 13.7$ Hz, 1H, CH_2CH), 3.03 (dd, $J = 4.9, 13.7$ Hz, 1H, CH_2CH), 3.77 (s, 3H, OCH$_3$), 3.99 (t,

J = 6.7 Hz, 2H, OCH_2), 4.61 (m, 1H, CH$_2$CH), 6.82 (d, J = 8.2 Hz, 2H, Ar-H), 7.14 (d, J = 8.2 Hz, 2H, Ar-H), 7.38 (m, 1H, Ar-H), 7.52 (d, J = 8.5 Hz, 1H, Ar-H), 7.64 (dd, J = 2.1, 8.5 Hz, 1H, Ar-H), 7.92 (d, J = 2.1 Hz, 1H, Ar-H), 8.00 (m, 1H, Ar-H), 8.62 (dd, J = 1.6, 6.1 Hz, 1H, Ar-H), 8.90 (d, J = 1.5 Hz, 1H, Ar-H); ^{13}C NMR (125.7 MHz, CDCl$_3$): δ 17.04 (SCH$_3$), 24.54 (Ar-CH$_2$), 26.84 (CH$_2$$CH_2CH_2$), 32.47 (CO$CH_2$), 34.06 (S$CH_2$), 35.43 ($CH_2$CH), 56.64 (O$CH_3$), 57.82 (CH$_2$$C$H), 76.06 (O$CH_2$), 107.17, 115.42, 115.55, 122.39, 124.99, 125.04, 129.67, 131.04, 131.21, 131.69, 132.27, 134.52, 136.37, 139.06, 149.33, 149.95, 150.75, 153.24, 160.12 (all C$_{arom}$), 172.86 (C=O), 174.33 (C=O). Anal. Calcd for C$_{31}$H$_{33}$Cl$_2$N$_5$O$_4$S (642.60): C 57.94, H 5.18, N 10.90. Found: C 57.90, H 5.24, N 10.83.

3.3. GGT1 and FT assays

Assays were carried out on black bottom 96-well plates and read on a Tecon micro plate reader. The assay system (100 μl) contained 50 mM Tris-HCl (pH 7.4), 10 μM GGPP (in case of GGT1 inhibition) or 10 μM FPP (in case of FT inhibition), 5 μM dansyl-GCVLL, 5 mM DTT, 5 mM MgCl$_2$, 10 mM KCl, 50 μM ZnCl$_2$, 0.04% *n*-Dodecyl β-D-maltoside and indicated concentration of compounds dissolved in 1 μl DMSO. All the mixtures were incubated at 30 °C for 5 min before use. The reaction was initiated by the addition of 500 ng of pure GGT1 or FT and the fluorescence was measured for 20 min (with readings taken every 1 min) at 30 °C with the excitation wavelength at 340 nm and the emission wavelength at 520 nm. Each measurement was performed in triplicates and the IC$_{50}$ values (concentrations resulting in 50% enzymic inhibition) were calculated using three independent measurements of five to seven different concentrations. GGTI-DU40 (Duke University) and FTI-277 (Sigma-Aldrich) were used as positive controls for GGT1 and FT inhibition, respectively.

3.4. Western blot analysis

MDA-MB-231 breast cancer cells were seeded at 6 × 10^4 cells/well of a 6-well plate 24 h before inhibitor treatment and incubated at 37 °C in 5% v/v CO$_2$. The total volume in each well was maintained to 2 ml. The inhibitor compounds dissolved in DMSO were added in 5 μM final concentration in each well, whereas in the control well the same volume of DMSO (10 μL of DMSO (0.5%) was added. After 48 h, cells were washed twice with cold PBS and lysed using cell extraction buffer 20 mM HEPES, pH 8.0, 1 mM EDTA, 3 mM dithiothreitol, 10 mM MgSO$_4$, 150 mM NaCl, 1% Triton X-100. The protein concentration was quantified using the Pierce BCA Protein Assay kit (Thermo Scientific). Protein samples (20−30 μg) were separated by 10% SDS-PAGE, transferred onto an Immun-Blot PVDF membrane (Bio-rad) and blotted with Rap1A antibody (Santa Cruz Biotechnology, Inc. CA). GGTI-DU40 was used as the positive control inhibitor, tubulin (Sigma) was used as the loading control for the immunoblot and visualized by Western Lightning-ECL (Millipore).

3.5. Cell proliferation assay

MDA-MB-231 breast cancer cells were cultured in 96-well microplates (5000 cells per well) for 24 h and then treated with compounds at different concentrations ranging from 2 μM to 32 μM for 48 h. The cytotoxicity of compounds in MDA-MB-231 cells was evaluated based on its effect on cell growth, which was determined by using CellTiter 96® Aqueous One Solution Cell Proliferation Assay (Promega, Madison, WI) at 48 h. Briefly, 10 μl of CellTiter 96 Aqueous One Solution Reagent was added into each well and incubated for 1 h at 37 °C in a humidified 5% CO$_2$ incubator. The absorbance measurement was done at 490 nm (Tecon Micro plate reader) and plotted in the graph using Prism. Each experiment was performed in triplicates and repeated three times. The cytotoxic effects of the extracts were estimated in terms of growth inhibition percentage and expressed as IC$_{50}$, which is the concentration of the compound, which reduces the absorbance of treated cells by 50% with reference to the control (DMSO treated cells).

3.6. Computational methods

The crystal structure of the GGT1 complexed with a GGPP Analog and a KKKSKTKCVIL peptide (PDB ID: 1N4Q) was employed in the docking calculations performed with Glide 6.2 (Schrodinger, LLC). Hydrogen atoms were added to the crystal structure, and the complex was submitted to a series of restrained, partial minimizations using the OPLS-AA force field within the "Protein and Ligand Preparation" module of Glide. Two docking runs were performed, the first keeping the peptide KKKSKTKCVIL and the second by removing the peptide prior to the docking calculation. To compensate for the fixed protein structure, which is not expected to be optimal for a particular ligand, the van der Waals radii for nonpolar ligand atoms were scaled by a factor of 0.8, thereby decreasing penalties for close contacts. Receptor atoms were not scaled. For the protein preparation, grid generation, and ligand docking procedures, the default Glide settings were used. The compound **2** was preprocessed with the Glide module "LigPrep", which ensured proper protonation and tautomerization states. The compounds were docked and scored using the Glide standard precision (SP) mode and subsequently the extra precision (XP) mode. In essence, Glide performs a thorough conformational search for a ligand; then it determines all reasonable orientations ("poses") for each low-energy conformer in the designated binding site. In the process, torsional degrees of the ligand are relaxed, though the protein conformation is fixed. The SP "scoring function" is applied to judge the poses by considering, for example, hydrophobic and electrostatic interactions, hydrogen bonding, steric clashes, desolvation and internal energy of the ligand, and possible trapped or bridging water molecules in the binding site. In XP mode, the poses are further relaxed by complete energy minimizations. The resultant more accurate structures provide a basis for more detailed evaluation of contributions from explicit water molecules in the binding site and hydrophobic interactions.

4. Conclusion

In conclusion, we synthesized a series of pyrazole based GGTIs, which are structural analogues of GGT1-DU40, a potent GGT1 inhibitor. All synthesized compounds were evaluated for their *in vitro* inhibition against GGT1 and FT enzyme, which revealed a clear trend of decreased inhibitory activity for propanamides (**6–16**) compared to butanamides (**2–5**). Among the tested compounds, **2** (IC$_{50}$ = 2.4 μM) exhibited the highest activity and turned out to be more active than the control compound **1** (DU40). The activity of **2** was slightly diminished, but was still comparable to **1**, when the fluoro moiety was replaced with a methoxy group to produce **5** (IC$_{50}$ = 3.1 μM). The screening results of *in vitro* inhibition against the FT enzyme revealed that all synthesized compounds are inactive at 100 μM, which suggests that they are selective inhibitors of GGT1. The efficiency of the synthesized compounds was further validated by western blot analysis in MDA-MB-231 cell line, which highlighted the high inhibitory cellular activity of **2** and **5** compared to the control compound GGTI-DU40 (IC$_{50}$ = 3.3 μM). The target compounds were also tested for the anti-proliferative efficacies against the MDA-MB-231 cell line, which revealed a 3-fold higher activity of **2** (IC$_{50}$ = 7.6 μM) compared to **1** (IC$_{50}$ = 23.0 μM). Molecular docking studies of **2** against the crystal structure of GGT1

revealed several hydrogen bonding interactions and π-π contacts between **2** and the binding pocket of GGT1. The optimized scaffold of **2**, showing increased potency, merits its in vivo investigation.

Acknowledgements

Appendix A. Supplementary data

Supplementary data related to this article can be found at http://dx.doi.org/10.1016/j.ejmech.2016.09.002.

References

[1] J. Colicelli, Sci. STKE 2004 (2004) RE13.
[2] S.F. Sousa, P.A. Fernandes, M.J. Ramos, Curr. Med. Chem. 15 (2008) 1478–1492.
[3] M.H. Gelb, L. Brunsveld, C.A. Hrycyna, S. Michaelis, F. Tamanoi, W.C. Van Voorhis, H. Waldmann, Nat. Chem. Biol. 2 (2006) 518–528.
[4] A.M. Winter-Vann, P.J. Casey, Post-prenylation-processing enzymes as new targets in oncogenesis, Nat. Rev. Cancer 5 (2005) 405–412.
[5] N. Berndt, A.D. Hamilton, S.M. Sebti, Nat. Rev. Cancer 11 (2011) 775–791.
[6] M. Malumbres, M. Barbacid, Nat. Rev. Cancer 3 (2003) 459–465.
[7] A.B. Jaffe, A. Hall, Annu. Rev. Cell Dev. Biol. 21 (2005) 247–269.
[8] E.A. Clark, T.R. Golub, E.S. Lander, R.O. Hynes, Nature 406 (2000) 532–535.
[9] A. Hakem, O. Sanchez-Sweatman, A. You-Ten, G. Duncan, A. Wakeham, R. Khokha, T.W. Mak, Genes Dev. 19 (2005) 1974–1979.
[10] R.J. Doll, P. Kirschmeier, W.R. Bishop, Curr. Opin. Drug Discov. Devel 7 (2004) 478–486.
[11] M.R. Philips, A.D. Cox, J. Clin. Invest.. 2007 (117) (2007) 1223–1225.
[12] A.K. Jogren, K.M. Andersson, M. Liu, B.A. Cutts, C. Karlsson, A.M. Wahlstrom, M. Dalin, C. Weinbaum, P.J. Casey, A. Tarkowski, B. Swolin, S.G. Young, M.O. Bergo, J. Clin. Invest. 117 (2007) 1294–1304.
[13] D.J.G. Mackay, A. Hall, J. Biol. Chem. 273 (1998) 20685–20688.
[14] F. Imamura, M. Mukai, M. Ayaki, K. Takemura, T. Horai, K. Shinkai, H. Nakamura, H. Akedo, Clin. Exp. Metastasis 17 (1999) 141–148.
[15] M.A. Chotani, K. Touhalisky, I.M. Chiu, J. Biol. Chem. 275 (2000) 30432–30438.
[16] J. Sun, Y. Qian, Z. Chen, J. Marfurt, A.D. Hamilton, S.M. Sebti, J. Biol. Chem. 274 (1999) 6930–6934.
[17] A. Vogt, J. Sun, Y. Qian, A.D. Hamilton, S.M. Sebti, J. Biol. Chem. 272 (1997) 27224–27229.
[18] H.C. Dan, K. Jiang, D. Coppola, A. Hamilton, S.V. Nicosia, S.M. Sebti, J.Q. Cheng, Oncogene 23 (2004) 706–715.
[19] M.A. Morgan, J. Wegner, E. Aydilek, A. Ganser, C.W. Reuter, Leukemia 17 (2003) 1508–1520.
[20] W.W. Stark Jr., M.A. Blaskovich, B.A. Johnson, Y. Qian, A. Vasudevan, B. Pitt, A.D. Hamilton, S.M. Sebti, P. Davies, Am. J. Physiol. 275 (1998) L55–L63.
[21] A. Kazi, A. Carie, M.A. Blaskovich, C. Bucher, V. Thai, S. Moulder, H. Peng, D. Carrico, E. Pusateri, W.J. Pledger, N. Berndt, A. Hamilton, S.M. Sebti, Mol. Cell Biol. 29 (2009) 2254–2263.
[22] S.M. Sebti, A.D. Hamilton, Oncogene 19 (2000) 6584–6593.
[23] J. Lu, K. Yoshimura, K. Goto, C. Lee, K. Hamura, O. Kwon, F. Tamanoi, PLoS One 10 (2015) e0137595.
[24] K.M. Sane, M. Mynderse, D.T. LaLonde, I.S. Dean, J.W. Wojtkowiak, F. Fouad, R.F. Borch, J.J. Reiners Jr., R.A. Gibbs, R.R. Mattingly, J. Pharmacol. Exp. Ther. 333 (2010) 23–33.
[25] (a) A. Vogt, Y. Qian, T.F. McGuire, A.D. Hamilton, S.M. Sebti, Oncogene 13 (1996) 1991–1999;
(b) M. Watanabe, H.D.G. Fiji, L. Guo, L. Chan, S.S. Kinderman, D.J. Slamon, O. Kwon, F. Tamano, J. Biol. Chem. 283 (2008) 9571–9579.
[26] N. Ullah, M. Mansha, P.J. Casey, Curr. Cancer Drug Targets 16 (2016) 563–571.
[27] (a) A. Abbas, M. Mansha, N. Ullah, RSC Adv. 6 (2016) 26104–26110;
(b) A.A.Q. Al-Shaheri, Z. Naturforsch 67b (2012) 253–262;
(c) N. Ullah, J. Enzyme Inhib. Med. Chem. 29 (2014) 281–291;
(d) N. Ullah, Med. Chem. 10 (2014) 484–496.
[28] J. Iqbal, N.D. Tangellamudi, B. Dulla, S. Balasubramanian, Org. Lett. 14 (2012) 552–555.
[29] O.P. Horlacher, R.C. Hartkoorn, S.T. Cole, K.-H. Altmann, ACS Med. Chem. Lett. 4 (2013) 264–268.
[30] S. A. Boyd, J. Demeese, F. S. Farouz, I. Gunawardana, I. C. Jacobson, R. A. Kasar, Y. Lehuerou, M. L. Lupher Jr, M. Mclaughlin, S. Miller, A. Thomas, E. D. Thorsett, R. Xu, M. Yanik, G. Zhang, WO2005016883, 2005.
[31] A.N. Hulme, E.M. Rosser, Org. Lett. 4 (2002) 265–267.
[32] M.P. Bosch, F. Campos, I. Niubo, G. Rosell, J.L. Díaz, J. Brea, M.I. Loza, A. Guerrero, J. Med. Chem. 47 (2004) 4041–4053.
[33] G.W. Hardy, L.A. Lowe, G. Mills, P.Y. Sang, D.S.A. Simpkin, R.L. Follenfant, C. Shankley, T.W. Smith, J. Med. Chem. 32 (1989) 1108–1118.
[34] M. Mansha, N. Ullah, K. Al-hooshani, Z. Naturforsch 71b (2016) 333–344.
[35] K. Guzow, R. Ganzynkowicz, A. Rzeska, J. Mrozek, M. Szabelski, J. Karolczak, A. Liwo, W. Wiczk, J. Phys. Chem. B 108 (2004) 3879–3889.
[36] N-N. Liu, S.-M. Zhao, J.-F. Zhao, G.-Z. Zeng, N.-H. Tan, J.-P. Liu, Tetrahedron 70 (2014) 6630–6640.
[37] C.L. Millington, A.J. Watson, A.S. Marriott, G.P. Margison, A.C. Povey, D.M. Williams, Nucleos. Nucleot. Nucl. 31 (2012) 328–338.
[38] M. G. Campbell, Z. Guo, F. F. Li, K. S. Rehder, J-P. Strachan, C. P. Viscardi, WO2004016592, 2004.
[39] J.A. Olsen, D.W. Banner, P. Seiler, B. Wagner, T. Tschopp, U. Obst-Sander, M. Kansy, K. Müller, F. Diederich, ChemBioChem 5 (2004) 666–675.
[40] J.S. Taylor, T.S. Reid, K.L. Terry, P.J. Casey, L.S. Beese, EMBO J. 22 (2003) 5963–5974.
[41] R.A. Friesner, J.L. Banks, R.B. Murphy, T.A. Halgren, J.J. Klicic, D.T. Mainz, M.P. Repasky, E.H. Knoll, M. Shelley, J.K. Perry, D.E. Shaw, P. Francis, P.S. Shenkin, J. Med. Chem. 47 (2004) 1739–1749.
[42] R.A. Friesner, R.B. Murphy, M.P. Repasky, L.L. Frye, J.R. Greenwood, T.A. Halgren, P.C. Sanschagrin, D.T. Mainz, J. Med. Chem. 49 (2006) 6177–6196.